Polymer Vol. 37 No. 12, pp. 2309–2316, 1996

0032-3861/96/$15.00 + 0.00

Morphological behaviour and instrumented dart impact properties of β-crystalline-phase polypropylene

S. C. Tjong*, J. S. Shen and R. K. Y. Li
Department of Physics and Materials Science, City University of Hong Kong, 83 Tat Chee Avenue, Kowloon, Hong Kong
(Received 11 October 1994; revised 22 February 1995)

Specimens consisting of high-purity β-phase polypropylene were prepared by adding a bicomponent β-nucleator consisting of equal amounts of pimelic acid and calcium stearate. Scanning electron microscopy (SEM), differential scanning calorimetry (d.s.c.), dynamic mechanical analysis and instrumented drop weight impact tests were used to characterize the morphology, thermal behaviour and the impact properties of the β-phase polypropylene. SEM examinations show that the β-spherulites exhibit a sheaf-like structure with no clear boundaries between them. This distinct spherulitic morphology results in a substantial improvement in the falling weight impact resistance. Fractographic analysis reveals that microfibrils and voids were formed in the fracture induction area of the β-form specimen. The greater impact strength observed in the β-form material is due to the larger energy dissipation which is associated with the formation of microfibrils. Furthermore, d.s.c. analysis showed that there is no $\beta \rightarrow \alpha$ phase conversion during the impact test. Copyright © 1996 Elsevier Science Ltd.

(Keywords: β-phase; impact strength; polypropylene)

INTRODUCTION

Isotactic polypropylene (PP) is known to exhibit several crystalline forms, namely the monoclinic α-form, the hexagonal β-form and the triclinic γ-form[1,2]. The α-form is the most stable and is also the most prevalent one. The β-form is observed only occasionally during crystallization and it appears as a minority constituent of the PP. Under special crystallization conditions or when selective β-nucleators are used, higher levels of the β-form can be produced. The microstructure and mechanical properties of the α-form PP have been investigated extensively. In contrast, fewer studies have been made on the mechanical behaviour of the β-form PP, particularly its impact properties.

Jacoby *et al.*[3] have produced different levels of the β-form PP by adding a small amount of a quinacridone dye nucleating agent. They reported that PP which contains high levels of the β-form exhibits lower values of the modulus and yield stress, but higher values of the impact strength and elongation at break. In addition to organic nucleating agents, mineral fillers such as wollastonite, carbonate, talc, etc. can also be used to produce various levels of β-form crystallinity[4,5]. Liu *et al.*[4] reported that the relative content of the β-form approaches 37% when 17.7 vol% wollastonite is added to PP. For the carbonate- and talc-filled PP homopolymer, the amount of β-phase crystallites in these samples is very low even when up to levels of 40 wt% mineral content. The relative amounts of the β-phase in carbonate- and talc-filled PP samples are 12 and 1.8%, respectively[5]. The presence of the β-phase crystallites improves the impact strength of PP substantially[5].

Recently, Shi and coworkers[6–9] reported that a high purity of the β-phase can be formed in PP by adding a specific bicomponent β-nucleator consisting of equal amounts of pimelic acid and calcium stearate. The relative β-phase content can reach as high as 94% by adding only 0.1 wt% of such β-nucleators[9]. They also pointed out that this high-purity β-form sample exhibits a lower yield strength but a higher impact strength than those of the α-form sample[7]. Tjong *et al.*[10] have conducted a preliminary study on the impact behaviour of such high-purity β-form material. They also confirmed that the β-form sample exhibits a much higher Izod impact strength than that of an α-form sample. The above behaviour is related to a difference in the spherulitic morphologies between the α- and β-crystallites. The β-spherulite exhibits a sheaf-like structure[10], whereas the α-spherulite consists of an aggregate of lamellae growing and branching from a central nucleus. This present paper aims to investigate the drop-weight impact behaviour of the β-phase PP prepared by adding a bicomponent β-nucleator. The results are compared with the impact behaviour of the α-phase PP. It is advantageous to use the instrumented dart impact test because it is capable of testing materials of almost any configuration at a wide range of velocities and hence it can enhance our understanding of the correlation between the fracture

* To whom correspondence should be addressed

resistance of the supermolecular structure of PP under these severe conditions.

EXPERIMENTAL

Materials and preparation

PP (Pro-fax 6501) with a melt flow index of 4 g per 10 min was supplied by Himont Inc. The β-nucleator used is a mixture of equal amounts of pimelic acid and calcium stearate. The PP powders were premixed with 0.1 wt% of β-nucleator in a twin screw Brabender machine. The cylinder temperature was kept constant at 230°C. Extrudates were subsequently cut into pellets by a pelletizer. Dog-bone shaped tensile bars (ASTM D638) were made from pelletized extrudates by using a Chen Hsong injection moulding machine (model JM4 MKII-C). The melt temperature was 240°C and the mould temperature was 50°C. The relative contents of the β-phase in the skin and core section of the injection moulded specimens are 54 and 92%, respectively, on the basis of wide-angle X-ray diffraction analysis[10]. These specimens were denoted as β-form PP. For comparison purposes, the tensile bars of pure PP were also injection moulded by using similar processing conditions; the latter were denoted as α-form PP.

Characterization techniques

Microscopy. Morphological studies were performed on an Hitachi scanning electron microscope (model S-530). The specimens were cut from the injection moulded bars, and then etched with an aqueous solution of $KMnO_4/H_2SO_4/H_3PO_4/H_2O$. A thin layer of gold was evaporated on the specimen prior to the SEM observations.

Differential scanning calorimetry (d.s.c.). Measurements were made on both α-form and β-form PP specimens by using a Perkin-Elmer thermal analysis system (model DSC-7) at a heating rate of 10°C min^{-1}. Indium and zinc standards were used for temperature calibration. The d.s.c. specimens were cut from the central gauge section of the injection moulded bars, at a distance of ~1.5 mm beneath the skin layer.

Dynamic mechanical analysis (d.m.a.). Dynamic mechanical tests of the injection moulded specimens were performed in a Du Pont dynamic mechanical analyser (model 986) at a fixed frequency of 1 Hz. The temperature range of study was from −150 to 150°C.

Falling drop weight impact tests. Rectangular specimens with dimensions of 125 × 13 × 3.3 mm^3 for the impact tests were prepared from the gauge section of the injection moulded tensile bars. A Ceast Fractovise drop weight impact system was used to conduct the Charpy impact tests. The impactor was equipped with an instrumental tup and the signal was fed to a data acquisition board in a spectrum system computer. The mass of the striker was 3.164 kg and the free clearance was 95.3 mm. The impact speeds employed were 0.76, 1.4, 2.2, 3.4 and 4.8 m s^{-1}, respectively. Ten specimens were tested at each speed and the average value was then reported. All impact tests were carried out at 20°C. The fracture surface of the various specimens was examined in a scanning electron microscope (JOEL JSM-820). Furthermore, d.s.c. measurements were also conducted in order to detect whether the $\beta \rightarrow \alpha$ phase transition process occurred during the impact tests. The d.s.c. specimens were prepared from the fracture surfaces of the impact notched specimens.

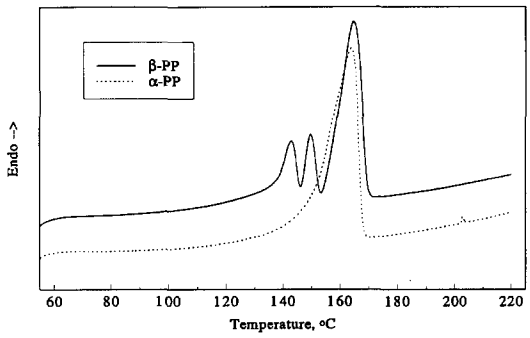

Figure 1 D.s.c. thermograms (first heating run) of the α- and β-form polypropylene specimens

RESULTS AND DISCUSSION

Melting behaviour

Figure 1 shows the d.s.c. traces (first heating run) of the α- and β-form PP specimens, respectively. It is apparent from this figure that the β-form PP exhibits three endothermic melting peaks, whereas the α-form PP only exhibits a single endothermic peak at ~164°C. Shi *et al.*[11] indicated that the first two peaks of the β-form PP are caused by melting of the original β_1-phase and subsequent recrystallization to produce a more stable structure (β_2) during scanning, while the last peak is associated with the melting of the original and recrystallized α-phase crystals. The structure of β_1 is relatively less ordered than that of β_2 on the basis of X-ray diffraction analysis, i.e. the β_1 crystal has a lower order of chain packing along the chain direction[12]. The relative proportions of the β_1- and β_2-phases formed in PP depend significantly on the content of the β-nucleator added and the crystallization temperature[9,12]. On the other hand, such double melting phenomenon of the β-phase is not observed in either mineral-filled PP[4] or in quinacridone-dye-containing PP[3]. Furthermore, it should be noted that the $\beta \rightarrow \alpha$ phase transition can take place in PP during thermal treatment at a temperature above 145°C and this transition depends on the structure of the β-nucleator that is added[12]. Thus the d.s.c. curve of high-purity β-form PP is complicated by the presence of the β_1- and β_2-phases and a $\beta \rightarrow \alpha$ phase transition process.

Dynamic mechanical analysis

Figures 2a–c show the dynamic mechanical spectra of the α-PP and β-PP specimens. Three transitions are observed at ca. −75, 14 and 81°C for the α-form PP sample. The relaxations at ca. −75 and 81°C appear as shoulders in the tan δ *versus T* curve. Liu *et al.*[4] reported that there exists three relaxation peaks in the loss factor (tan δ) *versus* temperature spectrum of the α-form PP specimen, i.e. at −40, 10, and 75°C, denoted by α-, β- and γ-relaxations. Jacoby *et al.*[3] also reported that there are three major transitions for the β-form PP, and the

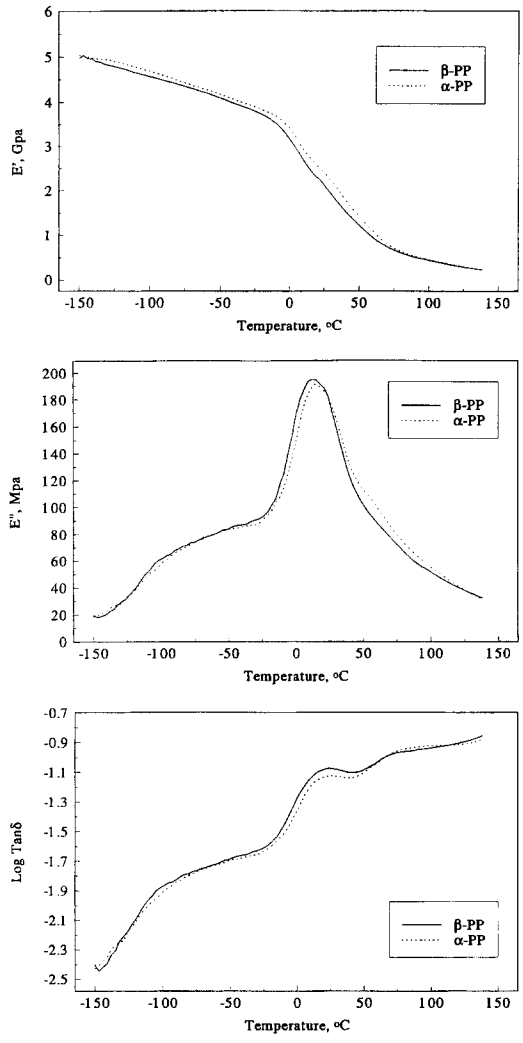

Figure 2 Dynamic mechanical spectra for the α- and β-form PP specimens showing variations of (a) storage modulus, (b) loss modulus and (c) loss factor (tan δ) with temperature

loss peaks are located at ca. −75, 0, and 80°C. The loss peaks at −75 and 80°C also appear as shoulders in the spectrum[3]. For the β-form PP specimen, the transition as ca. 13°C is identified as the glass transition (T_g). The α- and β-form PP specimens exhibit an almost identical T_g transition temperature and intensity of secondary transition peak. From *Figure 2a*, it can be seen that the storage modulus is slightly lower in the β-PP specimen that in the α-PP specimen. Such behaviour is similar to that of the static tensile modulus, as reported previously[10]. However, Jacoby *et al.*[3] reported that the storage modulus of PP appears to increase with an increasing β-content. The discrepancy in the storage modulus results is possibly due to the difference in the β-content between their specimens and ours.

Spherulitic morphology

Figures 3a–d show scanning electron micrographs of the morphology of the β-form PP spherulites, whereas *Figure 3e* shows the spherulite morphology of α-form PP. These micrographs reveal that the addition of β-nucleator to PP leads to a substantial decrease in the size of the spherulites. The β-spherulites consist of parallel-stacked lamellae[1]. The lamellae tend to cluster into bundles, with these being separated from one another by

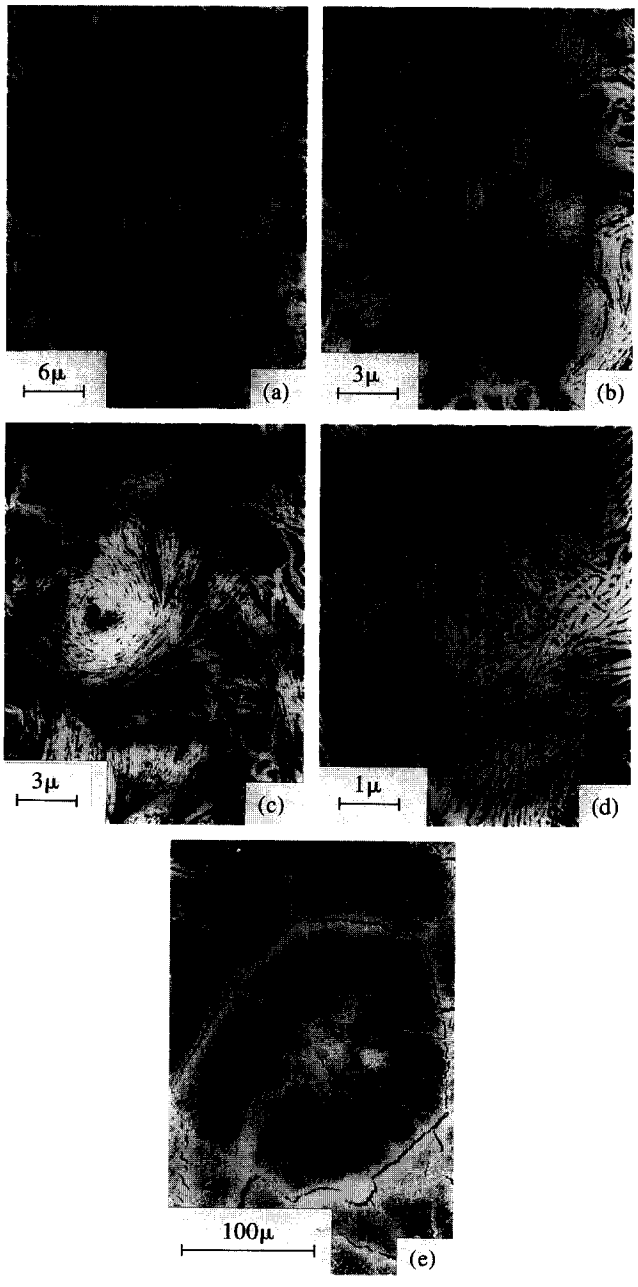

Figure 3 Scanning electron micrographs of the β- and α-form PP specimens. Micrograph (a) shows the predominant fine β-spherulites with few α-spherulites present, with enlarged pictures of the β-spherulites showing (b) a sheaf-like structure, (c) a spiral structure, and (d) bundles of chain folded lamellae. Micrograph (e) shows the morphology of the α-spherulites

the amorphous regions. From *Figure 3d*, it is evident that these fine β-spherulites exhibit a sheaf-like structure, and the boundaries between the spherulites are hardly distinguishable. Moreover, it can be seen that bundles of lamellae of neighbouring spherulites tend to cross each other (*Figure 3d*) and some of these bundles tend to grow spirally (*Figure 3c*). Shi *et al.*[13] reported that the β-spherulites develop initially as rod-like structures and then by branching of the lamellae, which finally evolve into sheaf-like structures. In this case the spherulite is formed from one crystal via an unidirectional growth mechanism. The spherical shape is attained through continuous branching and fanning via the intermediate stage of sheaves. However, the α-spherulites consist of an

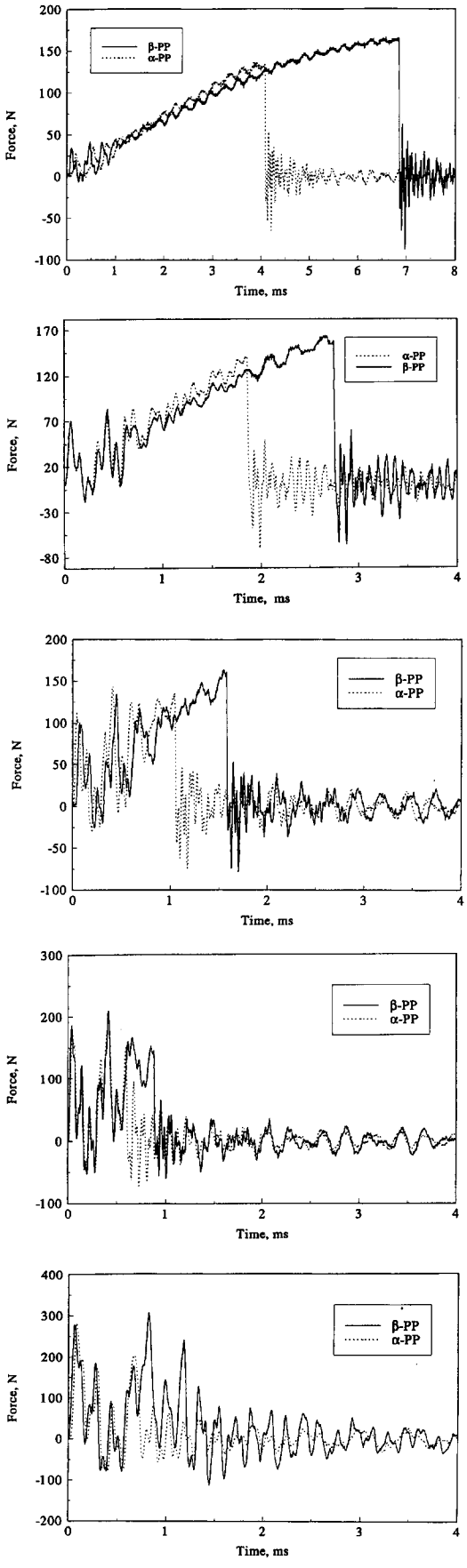

Figure 4 Load-time traces of the α- and β-form PP specimens impacted at a velocity of: (a) 0.76; (b) 1.4; (c) 2.2; (d) 3.4; (e) 4.8 m s^{-1}

aggregate of chain folded lamellae growing from a central nucleus. Different crystals nucleate separately during crystallization and the spherulites that are thus developed have distinct boundaries. These boundaries are weak sites in the polymer as failure of the PP is often initiated at these places.

It is generally known that the spherulitic microstructure plays a key role in controlling the fracture behaviour and the mechanical properties of polymers. The mechanical responses to tensile yielding differ substantially between the α- and β-spherulites. Tensile deformation of α-form PP usually involves a necking process in which the initial randomly-oriented spherulitic structure is converted into a highly oriented one. However, the β-form PP exhibits more homogeneous deformation without obvious necking formation during the drawing process[10]. Furthermore, the β-form PP specimen has a slightly lower yield strength than that of the α-form PP. The β-form PP specimen begins to whiten beyond yielding, and it then becomes completely whitened with further drawing, whereas the α-form PP exhibits partial stress whitening beyond yielding. This stress whitening is caused by the formation of numerous voids originating from a volume contraction[14] associated with the $\beta \rightarrow \alpha$ transformation during drawing as the crystallite density of the β-form (0.921 g cm^{-3}) is lower than that of the α-form (0.936 g cm^{-3}). Recently, Shen and Ren reported that numerous microcrazes are formed in a β-form PP specimen immediately after yielding[15].

Impact properties

Figures 4a–e show typical load–time curves of the α-PP and β-PP specimens impacted at different speeds. For all of the specimens the absorbed energy is the integral of the area under the force–time curve and is automatically determined by the instrument. The falling dart impact strength of the α-PP and β-PP specimens as a function of velocity is shown in *Figure 5*. Interestingly, high impact energy values are obtained for the β-PP specimen, particularly at a low impact speed of 0.76 m s^{-1}. In other words, the β-PP specimen demonstrates the best impact resistance, requiring nearly twice the energy to fracture the specimen at an impact speed of 0.76 m s^{-1} compared with that at 4.8 m s^{-1}. Therefore, increasing the dart speed to 4.8 m s^{-1} tends to diminish the microstructure-related difference in the impact response.

From *Figure 4*, it can be seen that secondary high-frequency oscillations were superimposed on the main force–time curves. The relative magnitude of the secondary oscillations over the main force–time curves become more predominant as the impact velocity increases. The nature of these oscillations has been addressed by a number of investigators[16–18]. Essentially, this behaviour is associated with the dynamic effects arising from the motion of the specimen and the wave propagation within the loading instrument. They can cause serious errors in the determination of dynamic critical stress intensity factors as the maximum force will be mistaken. Beguelin and Kausch[16] have demonstrated a solution to this potential problem by the application of a damping technique aimed at overcoming dynamic effects. In our present analysis, the secondary oscillations do not cause significant errors in the impact energy determination.

Fractography

Both α-PP and β-PP specimens fracture in a macroscopically brittle mode under rapid rate of loading in the impact tests. Although fracture appears to take place in a macroscopically brittle manner for some thermoplastics, microscopic examination shows they have undergone a small amount of plastic deformation[19,20]. *Figures 6a* and *6b* show the fracture surfaces (at low magnification) of the α-PP and β-PP specimens after falling dart impact tests at an impact velocity of 0.76 m s^{-1}. These micrographs reveal that the fracture surfaces of both types of specimens are relatively smooth and are of brittle appearance. However, plastic deformation is localized in a region close to the notch tip of the impact specimen. This region is called the fracture induction area, and is where the material breaks in a ductile manner[21]. A schematic representation of the deformation zones observed ahead of the notch tip in PP is shown in *Figure 6c*.

Figures 7a and *7b* show the scanning electron fractographs near the notch tip of the α-PP specimens after the impact tests. It can be seen from these micrographs that the size of the fracture induction area of the α-PP specimen tested at the lower impact speed of 0.76 m s^{-1} is considerably larger than that tested at an impact speed of 4.8 m s^{-1}. Thus the α-PP specimen

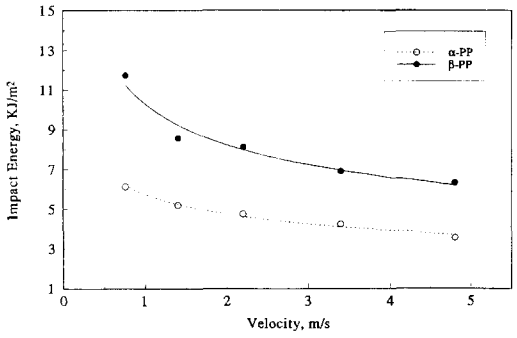

Figure 5 Instrumental falling weight impact strength of the α- and β-form PP specimens impacted at different speeds

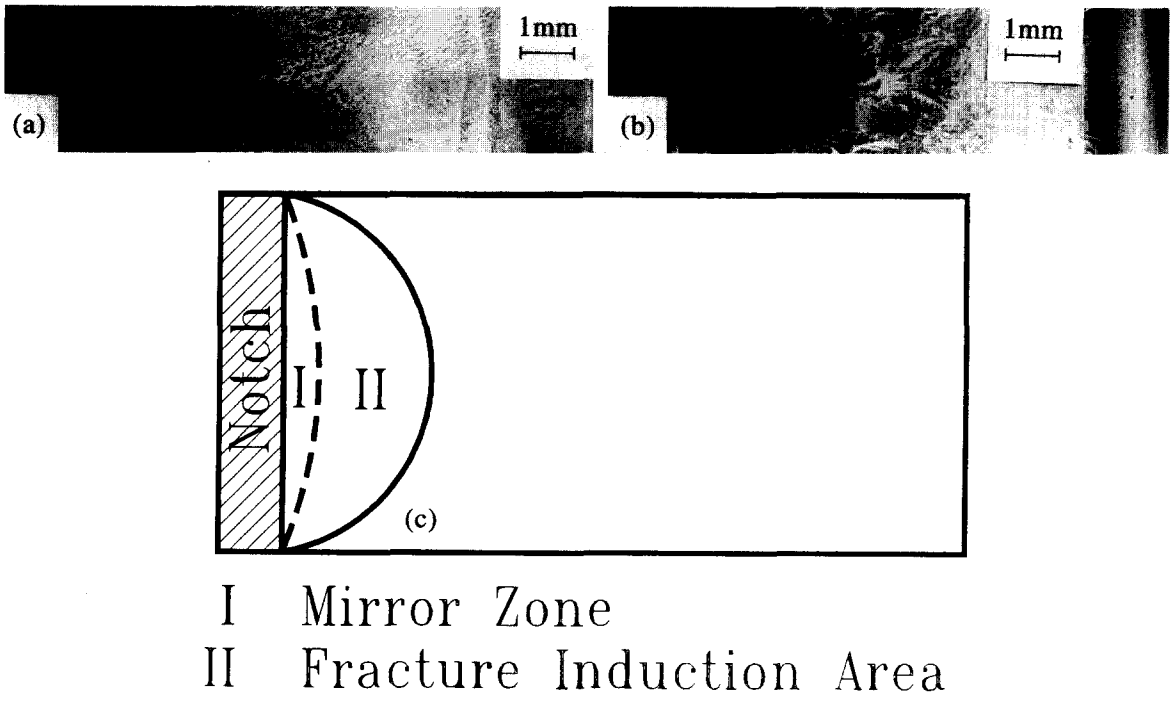

Figure 6 Low-magnification scanning electron fractographs of (a) α-form PP and (b) β-form PP, after impact tests. A schematic diagram of the deformation zones ahead of the notch tip is shown in (c)

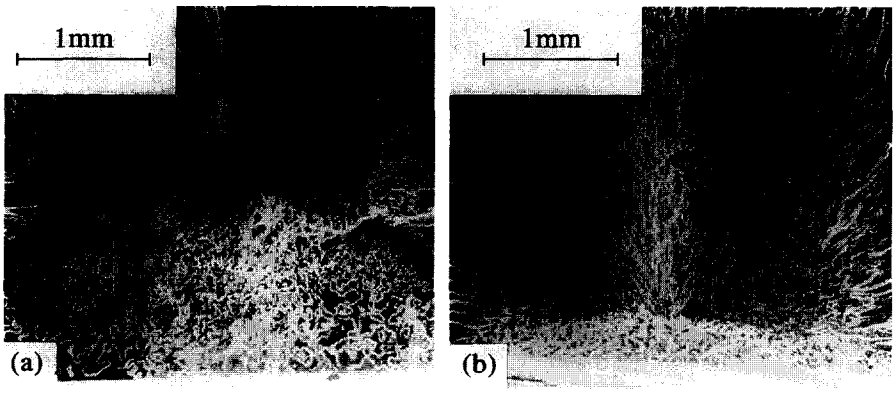

Figure 7 Scanning electron fractographs of the α-form PP impacted at (a) 0.76 and (b) 4.8 m s^{-1}

impacted at $0.76\,m\,s^{-1}$ with a larger fracture induction area exhibits a higher impact strength than that of the same specimen impacted at $4.8\,m\,s^{-1}$ (*Figure 5*). *Figure 8* shows a higher-magnification scanning electron micrograph of the fracture induction area of the α-PP specimen impacted at $0.76\,m\,s^{-1}$. As can be seen, this specimen experiences a relatively small amount of plastic deformation, which is associated with the formation of few microvoids. In contrast to the α-PP specimen, scanning electron micrographs show the existence of a high density of fibrils and microvoids in the fracture induction area of the β-PP specimen impacted at $0.76\,m\,s^{-1}$ (*Figures 9a* and *9b*). When the set impact speeds increase from 0.76 to $4.8\,m\,s^{-1}$, the density of microfibrils decreases dramatically in the fracture induction area of the β-PP specimen (*Figures 10a* and *10b*). Furthermore, the length of the fibrils is shorter than that shown in *Figure 9*. In this case, the impact resistance of the β-PP specimen decreases with increasing impact velocity, as shown in *Figure 5*.

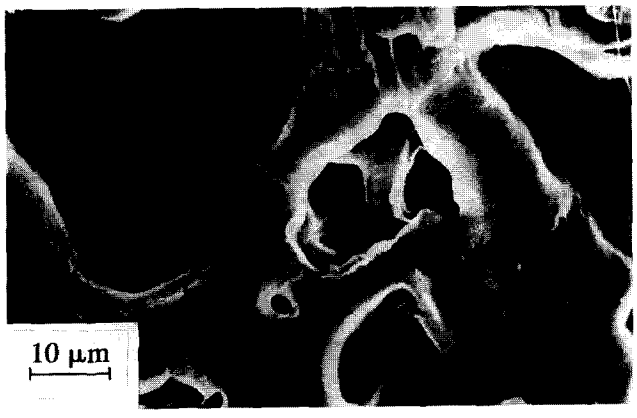

Figure 8 An enlarged picture of the fracture induction area shown in *Figure 7a*

In addition to the microscopic morphology difference in the fracture induction area between the α-PP and β-PP specimens, the microscopic features in the region away from the notch of both types of specimens are also different. *Figures 11a* and *11b* show scanning electron micrographs taken at the region furthest from the notch of the β-PP specimen. As can be seen, the topology of the fracture surface is very rough and uneven, and there is evidence for deformation in the form of microcracks and crazes. However, there appears to be less voiding and microcracking in this region for the α-PP specimen (*Figure 11c*). This implies that deformation occurs only in a localized region at the crack tip, and the energy absorbed by the α-PP specimen is confined to a small region when compared with the size of the specimen.

As mentioned above, the addition of a β-nucleator leads to much smaller spherulitic structures within PP. It is suggested that the improvement in impact properties can be partly explained in terms of these smaller spherulites[22]. Furthermore, the fractographic studies

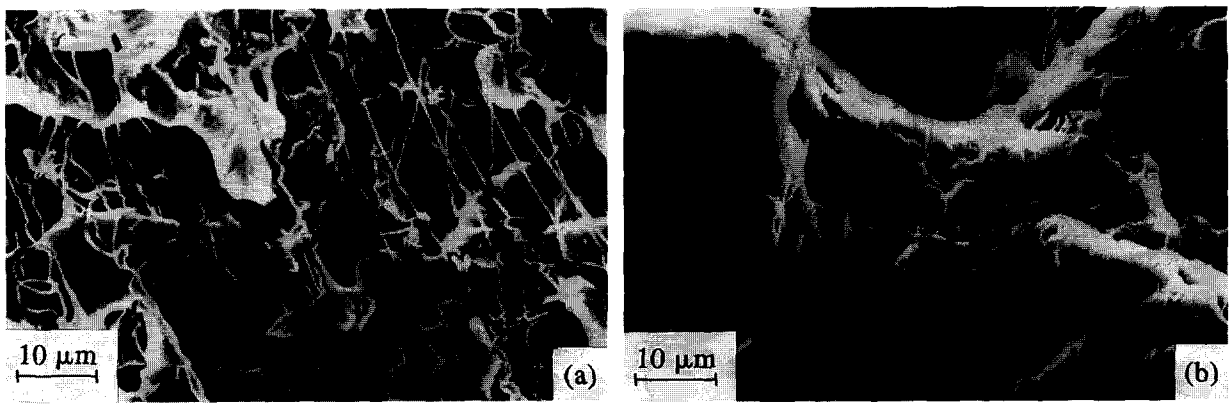

Figure 9 Scanning electron micrographs taken at regions near (a) the boundary between the mirror zone and fracture induction area, and (b) in the central region of the fracture induction area, for the β-PP specimen impacted at a velocity of $0.76\,m\,s^{-1}$

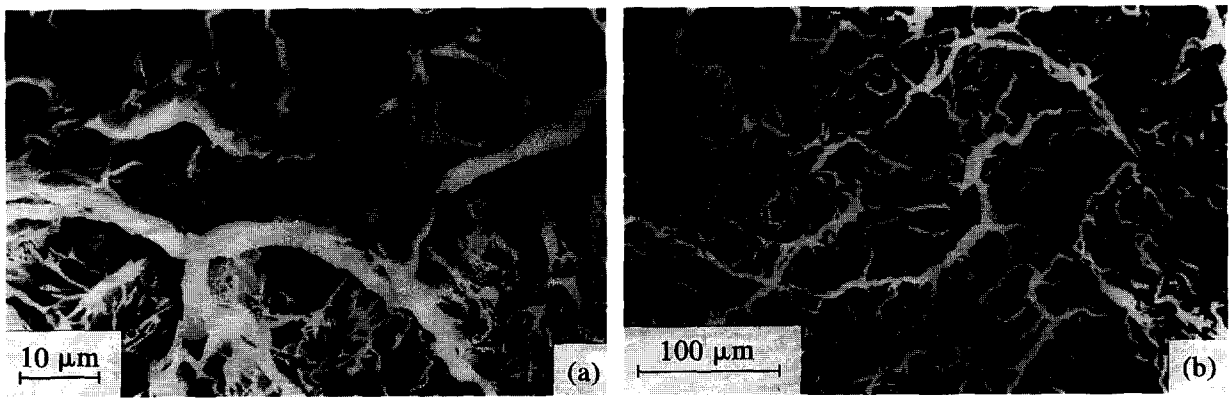

Figure 10 Scanning electron micrographs of the β-form PP specimen impacted at a velocity of $4.8\,m\,s^{-1}$, taken at regions near (a) the boundary between the mirror zone and fracture induction area, and (b) in the central region of the fracture induction area

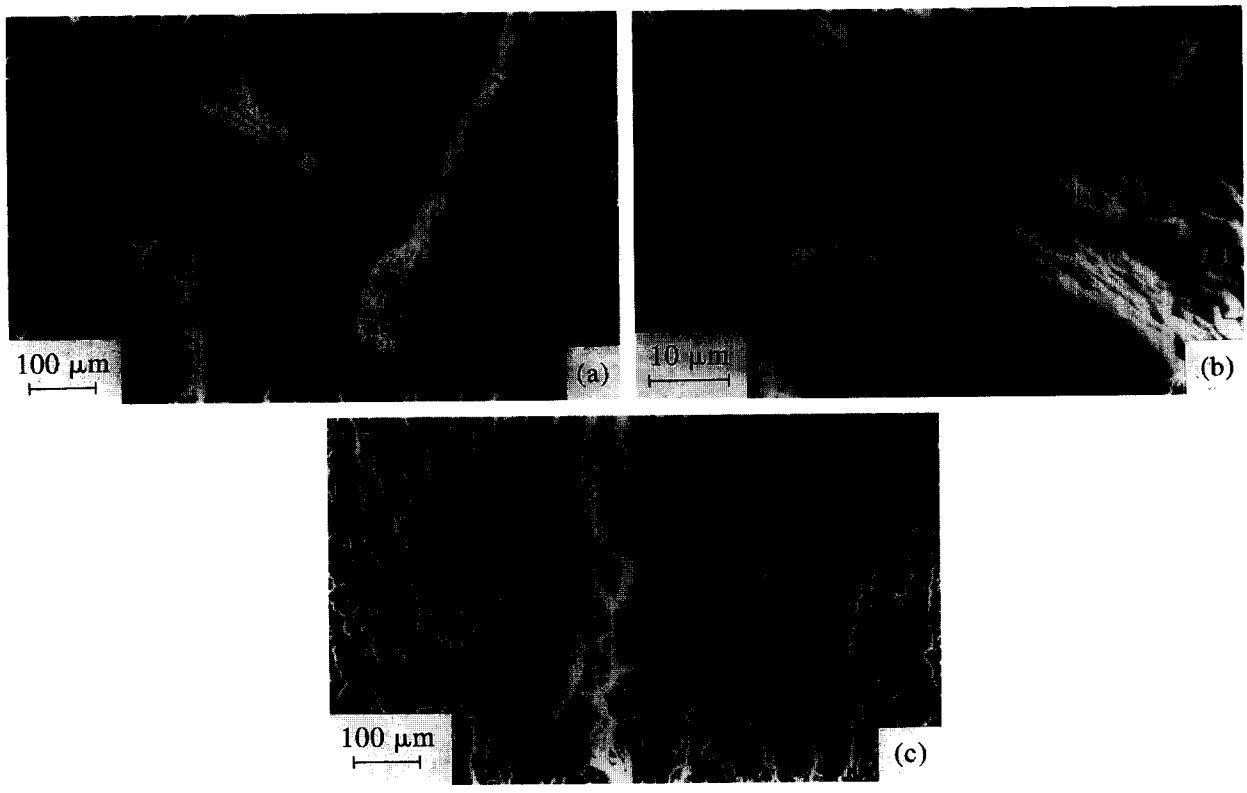

Figure 11 (a) Low- and (b) high-magnification scanning electron fractographs taken at the region furthest from the notch tip for the β-PP specimen impacted at the velocity of 0.76 m s^{-1}, with a corresponding fractograph of an α-PP specimen shown in (c)

reveal that the energy absorption of the PP strongly depends upon the supermolecular structure of PP. In the case of a β-PP specimen, an increase in impact toughness is associated with the formation of a fibrillated zone in the fracture induction area and microcracks in the region furthest away from the notch. The fibrillar structure presumably results from the transformation of the lamellar texture under plane strain failure at slow crack speeds. Such transformation occurs by the formation of small voids in the stacks of lamellae within the β-spherulites and the voids then grow into a fibrillar texture at the expense of the lamellae. The formation of microvoids during the plastic deformation of β-form polypropylene has been reported in the literature[23]. The micro-drawing of the β-PP matrix proceeds mainly by interlamellar slippage and chain slip[24]. Furthermore, the tie molecules that run through the amorphous phase of β-form PP are also aligned into tie-fibrils during the interlamellar slippage[14]. From *Figures 9a* and *9b*, the diameter of the microfibrils formed in β-form PP during impact tests is smaller than 0.1 μm. The length of the fibrils can be extended up to tens of μm long. It should also be noted that the β-form PP exhibits a lower yield strength than that of α-form PP[10] and fibrillation can occur more easily in β-form PP. It has been reported by some workers[25,26] that a fibrillated damage zone ahead of the notch can be initiated more easily in a lower-yield-stress material. Once the damage zone fibrillates, the subsequent initiation of a crack is difficult and more energy will be absorbed in the fibrillated zone[25,26].

From *Figure 2*, it is worth noting that the dynamic mechanical spectra provide little information on the fracture toughness of PP. The α-PP and β-PP specimens exhibit almost identical T_g transition temperatures and

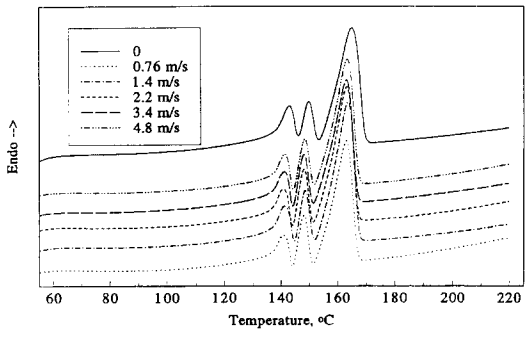

Figure 12 D.s.c. traces of a β-form PP specimen cut from the fracture surface after drop weight impact tests at various set impact speeds

intensities of the secondary transition peak. It is generally known that an increase in the impact toughness of certain polymers, e.g. polycarbonate, is related to the area and the peak intensity of the second transition[27,28]. A larger secondary-transition peak area generally leads to a higher impact toughness.

The β → α phase conversion

Finally, it has been reported that the β → α transition can take place by drawing or hot rolling of β-phase PP[3,24,29,30]. The amount of the β → α phase transition increased with increasing rolling temperature and draw ratio[24]. An increase in the impact energy is anticipated if such a phase transition occurs in the β-PP specimen during the impact tests. In this present work, there is no evidence for the occurrence of a β → α transition because the impact test time is relatively short. *Figure 12* shows the d.s.c. curves of a β-PP specimen cut from the fracture surfaces after falling dart impact

tests. It is apparent that the d.s.c. curves of the β-PP specimen after impact tests also show the presence of β_1 and β_2 peaks. The intensity of the β_2 peak appears to be slightly higher than that of the β_1 peak after the impact tests. This implies that there is a transition from a less-ordered β_1 crystal to an ordered β_2 crystal after the impact tests. Moreover, it can be seen that the α, β_1, and β_2 peaks shift to temperatures which are about two degrees lower than those of the β-PP specimen prior to the impact tests.

CONCLUSIONS

A high-purity β-form PP specimen was prepared by adding a bicomponent β-nucleator consisting of equal amounts of pimelic acid and calcium stearate. The morphology, impact properties and fracture characteristics of the β-form PP specimen have been investigated by using a scanning electron microscope and a standard V-notch Charpy drop weight test. SEM observations reveal that the β-spherulites exhibit a sheaf-like structure with no distinct boundaries between them. The instrumented falling weight impact tests show that the impact resistance of PP improves substantially by the addition of the β-nucleator. Furthermore, it is found that the impact strength of the β-PP specimen shows a pronounced decrease with increasing impact velocity. Scanning electron fractographs show that microfibrils and voids are formed in the fracture induction area of the β-form specimen. The greater impact toughness observed in the β-form PP specimen is due to the large energy dissipation which is associated with the formation of microfibrils.

ACKNOWLEDGEMENTS

This work was supported by a strategic grant from the City University of Hong Kong (Grant number 700–302), and was carried out while J. S. Shen was on leave from the Institute of Chemistry, Academia Sinica, Beijing, China.

REFERENCES

1 Norton, D. R. and Keller, A. *Polymer* 1985, **26**, 704
2 Varga, J. *J. Mater. Sci.* 1992, **27**, 2557
3 Jacoby, P., Bersted, B. H., Kissel, W. J. and Smith, C. E. *J. Polym. Sci. Polym. Phys. Edn* 1986, **24**, 461
4 Liu, J., Wei, Z. and Guo, Q. *J. Appl. Polym. Sci.* 1990, **41**, 2829
5 McGenity, P. M., Hooper, J. J., Paynter, C. D., Riley, A. M., Nutbeem, C., Elton, N. J. and Adams, J. M. *Polymer* 1992, **33**, 5215
6 Shi, G. and Zhang, J. *US Patent 5231126* 1993
7 Zhang, J., Shi, G., Cao, Y. and Wang, H. *Polym. Commun. China* 1986, **4**, 241
8 Shi, G. and Zhang, Z. *Thermochim. Acta* 1992, **205**, 235
9 Zhang, Z. and Shi, G. *Acta Polym. Sin.* 1992, **3**, 293
10 Tjong, S. C., Shen, J. S. and Li, R. K. Y. *Polym. Eng. Sci.* in press
11 Shi, G., Zhang, Z., Cao, Y. and Hong. J. *Makromol. Chem.* 1993, **194**, 269
12 Garbarcyzk, J. and Paukszta, D. *Colloid Polym. Sci.* 1985, **263**, 985
13 Shi, G., Zhang, Z. and Qui, Z. *Makromol. Chem.* 1992, **193**, 583
14 Zhang, Z. and Shi, G. *Polymer* 1994, **35**, 5067
15 Shen, J. and Ren, H. *J. Chin. Electron Microsc. Soc.* 1993, **4**, 342
16 Beguelin, P. and Kausch, H. H. *J. Mater. Sci.* 1994, **29**, 91
17 Adams, G. C., Bender, R. G., Crouch, B. A. and Williams, J. G. *Polym. Eng. Sci.* 1990, **30**, 241
18 Zanichelli, C., Rink, M., Pavan, A. and Ricco, T. *Polym. Eng. Sci.* 1990, **30**, 1117
19 Friedrich, K. and Karger-Kocsis, J. in 'Fractography and Failure Mechanisms of Polymers and Composites', (Ed. A. C. Roulin-Moloney), Elsevier, New York, 1989, p. 437
20 Hourston, D. J., Lane, S. and Zhang, H. Z. *Polymer* 1991, **32**, 2215
21 D'Orazio, L., Mancarella, C., Martuscelli, E., Slicotti, G. and Massari, P. *Polymer* 1993, **34**, 3671
22 Karger-Kocsis, J., Kallo, A., Szafner, A., Bodor, G. and Senyei, Z. *Polymer* 1979, **20**, 37
23 Chu, F., Yamaoka, T., Ide, H. and Kimura, Y. *Polymer* 1994, **35**, 3442
24 Yoshida, T., Fujiwara, Y. and Asano, T. *Polymer* 1983, **24**, 925
25 Channel, A. D. and Clutton, E. Q. *Polymer* 1992, **33**, 4108
26 Huang, Y. L. and Brown, N. *Polymer* 1992, **33**, 2989
27 Nielsen, L. E. 'Mechanical Properties of Polymers', Van Nostrand Reinhold, New York, 1962
28 Ke, Y., Ma, Z., Pan, P. and Shen, J. *Polym. Mater. Sci. Eng. (China)* 1992, **1**, 56
29 Asano, T., Fujiwara, Y. and Yoshida, T. *Polym. J.* 1979, **11**, 383
30 Fujiwara, Y. *Polym. Bull.* 1987, **17**, 539